Computer Networks 185 (2021) 107747

Contents lists available at ScienceDirect

Computer Networks

journal homepage: www.elsevier.com/locate/comnet

Ant Colony Optimization-based distributed multilayer routing and restoration in IP/MPLS over optical networks

Kelvin Santos Amorim, Gustavo Sousa Pavani *

Centro de Matemática, Computação e Cognição – Federal University of ABC (UFABC), Av. dos Estados, 5001. Santo André-SP, CEP: 09210-580, Brazil

ARTICLE INFO

Keywords:
Ant Colony Optimization
Adaptive routing and wavelength assignment
IP-over-optical
Traffic grooming
Distributed multilayer provisioning and restoration

ABSTRACT

The management of multilayer networks is often a complex task, since each layer is typically independently operated and maintained, and there is a lack of shared network resource knowledge between layers. In this work, we have illustrated that Ant Colony Optimization (ACO) algorithms can be a suitable solution for coordinated management of disjoint IP and optical layers with limited or no visibility between the control planes of each layer. ACO algorithms are used to achieve fully-distributed multilayer routing policies in IP-over-optical networks. Simulations have demonstrated that ACO-based policies can achieve lower levels of blocking probability and higher levels of restorability for IP connections compared to fixed-alternate routing policies in almost all cases. This better performance is achieved with only small increases in the connection setup and restoration times, and without requiring a significant amount of communication overhead.

1. Introduction

Intelligent optical transport networks have advanced control planes to support fast and flexible circuit provisioning, and improved survivability [1]. They offer important management capabilities to fulfill the needs of service providers, allowing for the efficient transport of IP traffic.

Due to the traditional separation between the IP and the optical transport layers, solutions that take into consideration a unified control plane for both IP and optical layers may have limited practical applicability. Moreover, network providers are reluctant to share detailed information about their topologies or resource usage to their customers [1].

In addition, full visibility of the topology and up-to-date information about network resource utilization are frequently required for most of the proposed multilayer routing approaches, which are based on centralized databases and/or algorithms [1].

In effect, most adaptive routing algorithms [2] assume an accurate global knowledge of the network state. However, when the traffic is highly dynamic, the GMPLS link-state update mechanism cannot have accurate information on each available wavelength in the network without placing an enormous processing load on the network elements or without consuming significant signaling capacity of the network [3].

On the contrary, in fully distributed managed networks, the route calculation and the reservation of network resources are performed in a hop-by-hop fashion [4]. A given node examines a setup request based on its local state knowledge. If the node has enough resources to satisfy the request, it determines the next hop for the request path. Otherwise, backtracking is used to find a new candidate path.

Therefore, by using only local information, distributed controlled networks may provide improved scalability and reliability when compared to centrally managed networks as they do not require a centralized entity or network state database, which can be seen as a single point of failure, to provision or recover connections.

In this context, Ant Colony Optimization (ACO) metaheuristics [5] can be a suitable candidate for the distributed control of networks [6]. ACO was originally proposed to find the minimum cost path in a graph, where artificial ants can construct very effective solutions by using their memory and by implementing a limited set of behaviors. In communication networks, where the topology and the cost of its links can dynamically change due to traffic fluctuations, congestion, and failures, typically there is no known polynomial solution to tackle the dynamic routing problem. Even though, ACO can also be used to adaptively manage the network in an effective manner. For this reason, ACO-based algorithms have been applied in a great number of routing problems [6–8], including optical networks [9–14].

The goal of this paper is to present fully distributed multilayer routing policies based on the ACO metaheuristics as reliable solutions for on-line cross-layer connection provisioning and recovery in IP/MPLS-over-optical networks. The proposed routing policies consider disjoint, on-line control for the optical and IP/MPLS layers.

ACO may mitigate two limitations commonly associated with fully distributed routing algorithms [4]: (i) lack of global optimality as

* Corresponding author.
E-mail address: gustavo.pavani@ufabc.edu.br (G.S. Pavani).

https://doi.org/10.1016/j.comnet.2020.107747
Received 17 February 2020; Received in revised form 12 November 2020; Accepted 14 December 2020
Available online 22 December 2020

routing decisions are made in isolation; and (ii) long, unpredictable setup times and potential thrashing due to backtracking.

Indeed, the distributed, self-organizing nature of ACO algorithms [8] makes them promising contenders for automated topology discovery and maintenance at the control plane of each network layer. Moreover, improved backtracking can be achieved by using crankback re-routing extensions [9,15,16] at each control plane to enhance the setup and recovery of connections.

The ant-based approach is one example of a distributed adaptive routing methodology. It is not purported here that it is necessarily the best, although prior works [9,17,18] have indicated it performs well even in the presence of inaccurate routing information [16].

As noted in [19], the majority of recent work in the literature related to multilayer networks does not account for dynamic traffic and survivability. Also, most studies do not take into consideration the limitations imposed by the amount of network information exchanged by the routing policies or by the management of different administrative domains at each network control plane.

For example, in [20] and [21], the authors first introduced an integrated multilayer routing policy, which requires full knowledge of the network state in every node; it is acknowledged that this type of strategy poses important scalability issues. Consequently, they propose another policy that requires only network resource information for both layers at the source node to overcome this problem. However, even limited amounts of information sharing between layers may raise concerns about scalability in large-scale networks. In [22], the proposed algorithm (CAPA_AUG) requires the number of available wavelengths on every physical link. As a consequence, the wavelength availability information has to be flooded in the network by the routing protocol, which scales in proportion to the square number of the network nodes.

Nevertheless, the coordinate management of the IP layer and the optical transport layer can overcome the constraints dictated by the lack of integration between those layers while avoiding unnecessary duplication of management functions [1]. Thus different forms of interaction and coordination for the network layers are presented in this paper, resulting in different multilayer routing policies.

The main contribution of this paper is to demonstrate that the ACO algorithm can effectively manage a multilayer network, achieving much lower levels of blocking probability and higher restoration rates compared to the fixed-alternate approaches while not resulting in much higher setup and restoration times or requiring significant communication overhead in the network. Indeed, these important metrics were not covered in [18]. Moreover, in addition to simulating the same topology of [18] but with the double number of wavelengths, a different and more representative network topology from [18] is also considered in this work. Lastly, the assessment of the influence of: (i) the number of IP router ports; (ii) the preference for using the optical layer first; (iii) the resource utilization at each layer; and (iv) the restoration behavior of each policy in the optical layer are also contributions of this work.

Indeed, simulations are carried out to evaluate the performance of the ACO-based multilayer routing policies compared to traditional fixed-alternate [2] multilayer policies by considering normal operation and also failures of the network. The simulation results show that, in contrast to fixed-alternate approaches, which need some type of routing information across the optical layer to achieve better performance, ACO-based routing policies can obtain low levels of blocking probability and high survivability in case of failures, even if the control planes of IP and optical layers are completely isolated and separated. Besides, for ACO-based policies that use optical network resource information to reach a decision, only local information at the source node is sent to the IP client layer in order to avoid scalability issues.

The remainder of the paper is organized as follows. Firstly, we discuss the multilayer network architecture used throughout this work in Section 2. In Section 3, we present the Ant Colony Optimization proposal for distributed routing and restoration in multilayer networks. We propose the multilayer routing policies in Section 4, detailing the simulations carried out for assessing them in Section 5. The results obtained through simulations are shown and discussed in Section 6. Finally, in Section 7, conclusions are drawn.

2. Network architecture

The network architecture in this work consists of IP/MPLS routers attached to an optical network backbone. In the remainder of this work, we do not distinguish between IP and IP/MPLS, referring to it simply as IP. The optical network offers connectivity to the IP routers in the form of transparent lightpaths.

We consider two interconnection models for the control plane: overlay and augmented [23]. In both cases, there is a distinct control plane instance at each network layer. However, in the case of the augmented model, it is assumed that the IP layer can obtain routing information from the optical layer, but it cannot obtain the entire knowledge of the optical layer topology.

Indeed, it is current practice to independently manage the optical transport and the IP layers [1], since the network may not be operated by a single service provider or by a single organization within a service provider. For this reason, the peer model, which considers a single instance of the control plane, is not considered in this work.

The IP layer requests services to the optical layer via a User–Network Interface (UNI). The control between nodes at the same network layer is realized via a Network–Network Interface (NNI).

The set of all lightpaths established at the physical topology (PT) is commonly referred to as the virtual topology (VT). The virtual topology is the topology seen by routers at the IP layer, where a lightpath is seen as a one-hop, virtual link between two IP routers.

We consider that a wavelength selective cross-connect (WXC) [23] has in-fiber, out-of-band control channels interconnecting them. However, two IP routers can only exchange control information at the IP layer if there is an established lightpath between them, in an in-band fashion. Thus the virtual topology also defines the IP router neighborhood in the control plane of the IP layer.

Finally, we consider that the network control planes are based on the GMPLS standard [1,9], which allows for the integrated management of different network technologies, including packet and optical switching. Therefore, UNI and NNI signaling are realized using RSVP-TE messages. Also, protocol extensions for crankback signaling [9,15] are supported at all network nodes.

3. Ant colony optimization

The class of algorithms known as Ant Colony Optimization is inspired by the foraging behavior of natural ants. By laying down chemical markers, which are called pheromones, they can develop trails connecting the nest to different food sources. This type of indirect communication based on modifications of the environment to stimulate subsequent actions is referred to as stigmergy [24].

Correspondingly, ACO algorithms are based on artificial stigmergy, where artificial pheromone levels have positive or negative feedback according to the solution quality seen by the ants. Since these levels contain information from previous solutions to the problem, they can be explored collectively by the ants to improve the solution [5].

Due to the artificial stigmergy, ACO exhibits Swarm Intelligence (SI), which is a property of limited, non-intelligent individual agents to display intelligent and self-organizing behavior collectively [8,25].

AntNet [17] is an algorithm based on ACO metaheuristics whose main application is routing in telecommunication networks. Indeed, it has proved to be an effective approach for routing packets in packet-switching networks [17], being competitive with other state-of-the-art algorithms.

The original AntNet algorithm was later adapted to be used in optical networks, such as those based on wavelength routing [9] and Optical Packet Switching (OPS) technology [26]. Instead of using the delay introduced at each hop as the metric for routing as in [17], these adaptations consider the number of traversed hops, which are stored in the ants' memory. Hence, each ant carries the identification of each node it traverses.

In addition to the artificial ants and their memory, there are two data structures to be maintained at each node i of the network [9,17]:

1. A pheromone-routing table $\mathcal{T}^i$, which is a matrix representing the pheromone level τ^i_{nd}, for a given destination node d and neighbor node n. The pheromone level estimates the goodness or probability of reaching a destination d given a neighbor node n as the next hop.
2. A statistical parametric model $\mathcal{M}^i$, which maintains distance estimates for each destination node d in the network. These distance estimates include the average path length μ_d, the standard deviation of the path length σ_d, and E_d, which is the shortest length of the paths that have been traversed by the ants, within the non-sliding window of w observations. The number of values in the window is calculated as $w = 5(c/\eta)$ [17], where $c \in (0, 1]$ and η is the factor of the exponential model used to update $\mathcal{M}^i$, which weighs the number of the most recent observations that will influence the mean.

These data structures store local state information and they can be considered a long-term memory of different aspects of the routing process [17]. Ants continuously probe the current state of the network and update the pheromone-routing table and the statistical parametric model of the nodes that they have traversed. They work as control messages exchanged by the nodes at the network's control plane, replacing the routing protocol while maintaining the signaling protocol essentially unaltered [9].

The solution construction process, i.e., the finding of feasible routes, and the updating of AntNet's data structures are summarized as follows [5,17]. At regular intervals ($1/R_{ants}$), an ant is sent from a random source node s to a random destination node d. This ant is called forward ant and it gathers the label of each node i where it traverses, putting it in its memory $V_{s\to i}$, which also serves as a tabu list.

The forward ant selects the next hop among the set of neighbor nodes $\mathcal{N}_i$ by using a probabilistic rule that accounts for the pheromone levels in each neighbor link and local information based on a heuristic function, which is problem-dependent.

The probability p^d_n for each neighbor node $n \in \mathcal{N}_i$ to be the next hop $(i + 1)$ is given by the equation [9,17]:

$$p^d_n = \begin{cases} \left(\frac{1}{1+\alpha}\right)\frac{\tau_{dn}}{\sum_{k\in T}\tau_{dk}} + \left(\frac{\alpha}{1+\alpha}\right)\frac{h_n}{\sum_{k\in T}h_k}, \forall n \in T \\ 0\ , \text{otherwise,} \end{cases} \tag{1}$$

where the left-most term relates to the pheromone level and the right-most term relates to the heuristic. α is used to control the emphasis between these two terms, and $T = \mathcal{N}_i \setminus V_{s\to i}$. If all neighbor nodes have already been visited (T is empty), the right-most term is ignored. In this case, after the selection of the next hop, all labels that belong to nodes of the cycle are removed from the ant's memory. Also, if the ant does not reach its destination node in a number of pre-established hops, it is discarded.

For wavelength-routed networks, the heuristic function h_n for node i accounts for the instantaneous availability of wavelengths on the link connecting to the next hop [9]:

$$h_n = \left(\frac{l^a_n}{W}\right)^f \tag{2}$$

where l^a_n is the number of available wavelengths on neighbor n, W is the total number of wavelengths deployed on the link and f is a power factor for enhancing the difference in the wavelength availability among neighbor nodes.

At the IP layer, we propose the use of the following heuristic function h^{IP}_n for node i:

$$h^{IP}_n = \left(\frac{b_n}{L}\right)^{f'} \tag{3}$$

where b_n is the available bandwidth between node i and neighbor node n, L is the total deployed bandwidth between nodes i and n, and f' is a power factor for enhancing the difference in the bandwidth availability among neighbor nodes. We assume that $f' = f$.

If a forward ant arrives at its destination, it becomes a backward ant and it returns to the source node using the same path followed when it was a forward ant. In its trip back to the source node, it will update the statistical parametric model, using an exponential model [9,17], and the pheromone routing table of the traversed nodes concerning the destination node and also update the statistically good sub-paths in the ant's memory.

An adaptive reinforcement r_d is calculated based on the goodness of the route found by the forward ant to reinforce the pheromone values [9,17] in the pheromone routing table. Also, a mechanism is employed to avoid stagnation of the pheromone values, limiting the maximum reinforcement value for a neighbor node [17]. Thus there is no need for an evaporation mechanism to avoid premature convergence [5].

At each traversed node, if a neighbor node m was the last visited node on the path traversed by the backward ant, it will receive a positive reinforcement in its pheromone value:

$$\tau_{dm} \leftarrow \tau_{dm} + r_d(1 - \tau_{dm}) \tag{4}$$

Conversely, the other neighbor nodes will receive a negative reinforcement of their pheromone values:

$$\tau_{dn} \leftarrow \tau_{dn} - r_d\tau_{dn}, \forall n \in \mathcal{N}_i, n \neq m. \tag{5}$$

Due to the use of network resource availability information for the heuristic function to route forward ants, which will in turn influence the pheromone levels deposited by the backward ants, the network can use longer paths that are less congested than the shortest ones. As a result, the network exhibits load-balancing capabilities [9], helping to lower the overall blocking probability of the network.

AntNet's main steps are summarized in Algorithm 1.

Algorithm 1: Outline of the AntNet algorithm.

```
At regular interval 1/R_ants, choose a random source node s
Node s creates forward_ant and send it to a random node d
/* At each node i                                          */
Solution_Construction(forward_ant,i)
    while not at node d do
        Discard forward_ant if maximum hop limit was reached
        Store node id i in forward_ant's memory
        Send forward_ant to the next hop using Eq. (1)
    forward_ant becomes backward_ant
    Send backward_ant to the previously visited node in its memory
    return
Updating_Data_Structures(backward_ant,i)
    while do
        Update the statistical parametric model
        Update the routing table using the adaptive reinforcement
        if not at source node s then
            Send backward_ant to the previously visited node in its
            memory
        else
            Discard backward_ant
            return
```

It is worth mentioning that the process of finding good routes in the network is fully distributed. Current pheromone values are used to guide the establishment of a Label-Switched Path (LSP) by the RSVP-TE signaling protocol. By using crankback re-routing extensions [9,15,16], a node can reissue an LSP setup to circumvent blocked resources until an alternate, feasible route is found. The number of re-routing attempts is limited at each node to mitigate the increase in setup latency and to prevent excessive network usage.

Also note that there is no need for global knowledge of the topology or central entities/databases, such as a Path Computation Element (PCE) and Virtual Network Topology Manager (VNTM), for path computation and topology management [1]. In effect, full topology knowledge may raise scalability issues in multilayer routing due to the high quantity of information needed to be exchanged among network nodes [3,20]. By contrast, in ACO algorithms, all information needed for network provisioning is local and can be discovered and monitored by the artificial ants.

As already mentioned, for the overlay and augmented interconnection models, we have separate control planes for the optical and IP layers. Therefore, we have two different and isolated ant colonies with their respective data structures: one for the optical layer and another for the IP layer.

4. Proposed multilayer routing policies

We assume that the network provider dynamically generates LSP requests f_{sd} from source node s to destination node d to fulfill bandwidth requests from users. At the ingress Label Edge Router (LER) nodes, the network combines these low-speed LSPs at the IP layer onto high-speed LSPs at the optical layer. This kind of multiplexing is often called traffic grooming [27,28].

The interaction between the optical and IP layers defines the multilayer routing policy of the network, which can also be called the grooming policy of the network [28]. In the rest of this paper, we adopt the formal framework definitions for multilayer routing policies that were presented in [28].

At the optical layer, we have a Routing and Wavelength Assignment (RWA) algorithm [2] in order to route and assign wavelengths for lightpaths, which we call Λ. We assume that Λ can only establish a single, direct lightpath between nodes s and d for each request due to limited knowledge of the topology. Similarly, at the IP layer, we have a routing algorithm, which will use the virtual topology, to find a route that has enough bandwidth available to transport each f_{sd}. This routing algorithm is called Ω.

Besides, we define the admission control criteria for coordinating the optical layer and the IP layer when an LSP request arrives at the network. These criteria are called Δ and they decide the sequential approach for managing LSP requests: invoke Λ or Ω first. The choice of what layer will try to accommodate a given request has a crucial role to minimize the blocking probability and maximize resource utilization.

Therefore, a multilayer routing policy G can be determined by the Λ and Ω algorithms and by the criteria Δ. Algorithm 2 outlines the coordination of the optical and IP layers for implementing a multilayer routing policy.

For this work, we consider different criteria Δ for the following fixed-alternate and ant-based Λ and Ω algorithms.

The multilayer routing policy IP-Layer First (ILF) [21,28,29] makes cautious use of the optical resources by always invoking Ω first. If that is not successful, then Λ is used. In either case, fixed-alternate routing is utilized [2], i.e., it has a pre-defined list containing the shortest-path, the second shortest-path, and so on. It is based on the overlay model as no routing information has to be exchanged between control planes.

By contrast, the Optical-Layer First (OLF) policy [21,28,29] makes aggressive use of the optical resources by always invoking Λ first. If that is not successful, then Ω is used. Similarly to ILF, it also uses Λ and Ω with fixed-alternate routing algorithms and it is also based on the overlay model.

The Direct-Connection First (DCF) policy, originally named Policy 2 in [27], looks for a lightpath between the source and destination nodes with enough capacity to serve f_{sd}. If such a lightpath exists, Ω is invoked to groom f_{sd} into the direct lightpath. Otherwise, Λ is invoked to try to establish a lightpath for accommodating f_{sd}. Again, the Λ and Ω algorithms use fixed-alternate routes. It uses the augmented model as the optical control plane has to inform the IP control plane that a suitable lightpath exists between the source and destination nodes.

Algorithm 2: Interworking of network layers in a multilayer routing policy.

```
MultiLayer_Routing_Policy(IP_request,G)
    Verify criteria Δ accordingly to policy G
    if Δ invokes Λ first then
        /* Optical layer starts first          */
        if Lightpath established then
            Invoke Ω to set up an IP LSP within the newly created
            lightpath
            return success
        else
            Invoke Ω to set up an IP LSP in the current virtual
            topology
            if IP LSP setup is blocked then
                return blocked
            else
                return success
    else
        /* IP layer starts first              */
        if IP LSP setup is blocked then
            Invoke Λ to set up a lightpath to accomodate the IP LSP
            if Lightpath established then
                Invoke Ω to set up an IP LSP within the newly created
                lightpath
                return success
            else
                return blocked
        else
            return success
```

The rationale for choosing ILF and OLF policies is that they are easy to implement and their behaviors are well-understood as they comprise the extreme cases of the coordination between the optical and IP control planes in the case of the overlay interconnection model. Correspondingly, for the augmented interconnection model, the DCF policy uses the virtual topology information to make an informed decision to coordinate the layers. Thus, by using limited information of the optical control plane in order to mitigate scalability issues, it tries to achieve a lower blocking probability than the considered overlay policies.

The ANT-ILF, ANT-OLF, and ANT-DCF policies use the same criteria Δ and the same interconnection model as ILF, OLF, and DCF, respectively. However, their Λ and Ω algorithms are based on ACO routing instead, as discussed in Section 3. This allows for a direct comparison of the routing efficiency of the Λ and Ω algorithms for these policies.

The Dynamic PArametric (DPA) policy [18] invokes Ω first for a request f_{sd}, if the observed path length at the IP layer, given by the entry μ_d of the Statistical Parametric Model from node s, is less than or equal to the maximum allowed hop number H. Otherwise, it invokes Λ first. This policy uses routing information obtained by the ants to make an informed decision to coordinate the control planes. Indeed, it tries to make conservative use of the optical resources by only trying to establish a new lightpath when the routes at the IP layer become longer than a pre-defined threshold. It also uses ACO-based routing for the Λ and Ω algorithms. It is based on the overlay model as no information has to be provided by the optical control plane.

Finally, the Dynamic PHeromone (DPH) [18] compares the pheromone levels at the source node s between the optical and the

Table 1
Summary of the fixed-alternate and the proposed ant-based multilayer routing policies used throughout this work.

Policy	Model	Admission control criteria Δ
ILF[a]	Overlay	Always invoke Ω first.
OLF[a]	Overlay	Always invoke Λ first.
DCF[a]	Augmented	Invoke Ω first, if $\mathcal{E}_{sd} \neq \emptyset$ and $\mathcal{E}_{sd}$ can transport f_{sd}. Otherwise, invoke Λ first.
ANT-ILF[b]	Overlay	Always invoke Ω first.
ANT-OLF[b]	Overlay	Always invoke Λ first.
ANT-DCF[b]	Augmented	Invoke Ω first, if $\mathcal{E}_{sd} \neq \emptyset$ and $\mathcal{E}_{sd}$ can transport f_{sd}. Otherwise, invoke Λ first.
DPA[b]	Overlay	Invoke Ω first, if μ_d for node $s \in \text{VT} \leq H$. Otherwise, invoke Λ first.
DPH[b]	Augmented	Invoke Ω first, if $\max(\tau^s_{nd} \in \text{VT}) > \max(\tau^s_{nd} \in \text{PT})$. Otherwise, invoke Λ first.

[a]Fixed-alternate.
[b]ACO.
VT = Virtual Topology, PT = Physical Topology.

IP colonies regarding the destination node d. It chooses Ω first if the highest value of pheromone for any neighbor can be found on the IP colony. Otherwise, the policy will invoke Λ first. A neighbor with a high concentration of pheromone can be a good indication of which layer is better to start the multilayer routing. It also uses ACO-based routing for the Λ and Ω algorithms. As information on the optical control plane is needed, an augmented model is used for this policy. Note that the level of pheromone is a simple scalar number and it does not require any topological information in contrast to the DCF and ANT-DCF policies.

For all policies, we consider that the RWA algorithm Λ uses the first-fit approach for the wavelength assignment sub-problem [9].

Note that, in contrast to the physical topology that has a single bi-directional link interconnecting two nodes, multiple bi-directional lightpaths can interconnect two IP routers at the virtual topology. Let us call $\mathcal{E}_{ij}$ the set of lightpaths that connect a node i to a node j on the graph representing the virtual topology. If there is more than one virtual link between nodes i and j that belongs to the route between s and d, Ω picks the first available virtual link (first-fit) in $\mathcal{E}_{ij}$ with enough capacity to satisfy f_{sd}. We assume that the virtual links are ordered by the time they were established in the network.

In conclusion, we present two multilayer algorithm classes in this work: fixed-alternate and ACO-based routing. Table 1 summarizes the multilayer routing policies used throughout the paper by presenting their interconnection model and their respective set of admission control criteria, which define the coordination between the optical and IP layers.

4.1. Survivability

In this work, we employ restoration as the recovery mechanism. Restoration is the process of recovering connections or routes affected by a failure using the available spare capacity of the network after the occurrence of the failure.

Coordination between optical and IP layers is necessary to provide efficient network survivability as a reaction to the occurrence of a single failure in the network [30].

Thus, for coordinating the restoration process, we employ bottom-up escalation, where the optical layer hands over the responsibility for recovery to the IP layer when it is clear that it cannot perform the recovery task [30,31]. Typically, upon failure detection, the optical layer starts the recovery immediately, but the recovery at the IP layer will be triggered by the expiration of a hold-off timer T_{HO}. The main advantage of this approach is that the recovery process is handled at the appropriate granularity, i.e., entire wavelengths affected by failure are handled first by the optical layer, while the IP layer only has to restore the portion of the affected traffic not recovered by the optical layer.

We consider end-to-end restoration without route pre-computation at both optical and IP layers, since it tends to be more efficient in terms of resource usage and more robust to multiple failures [9]. Indeed, a single node failure can be seen as a special case of multiple link failures. Besides, a single link failure at the optical layer can correspond with the simultaneous failure of multiple virtual links at the IP layer [30]. We also assume that the resources of a failed LSP are freed before the restoration process [9].

In fixed-alternate routing, we assume that the ingress node of the failed LSP has full knowledge of the new topology after failure due to the network's built-in notification and isolation of failures mechanism. In contrast, ACO-based routing can take advantage of local crankback information to recover from network failure even in the presence of inaccurate, out-of-date information in the pheromone routing tables [9,16].

5. Simulation

In order to evaluate the proposed multilayer routing algorithms, we use two topologies. The first one is the NTTNet (Nippon Telephone and Telegraph) backbone network [17,18]. It is composed of 57 nodes and 81 bi-directional links and is not a well-balanced network, with an average shortest-path length between all pairs of nodes equal to 6.5 hops and diameter equal to 14.

The other one is the CORONET Continental United States (CONUS) topology [3,32]. It is a hypothetical fiber-optic backbone network developed for use in researching large-scale DWDM networks. It is composed of 75 nodes and 99 bi-directional links, with an average number of hops equal to 6.9, an average nodal degree equal to 2.6, and an average link length equal to 400 km. The length of each link is calculated as the aerial distance between the end nodes of the link, inflated by 20% to represent terrestrial routing. We assume that a node introduces a delay equal to 0.4 ms [3] for processing an RSVP-TE message.

For this work, we have developed a custom event-driven simulation software, which is written in Java. It implements a distributed GMPLS control plane on both IP and optical layers, as discussed in Section 2.

Simulations are carried out with $W = 32$ wavelengths for NTTNet network and with $W = 16$ and 32 wavelengths per fiber for CORONET CONUS network. In all topologies, we consider one fiber per directional link. Unless otherwise noted, we assume that the maximum number of IP router ports is available to accommodate the W wavelengths at each link.

The dynamic traffic model assumes a Poisson distribution for the IP requests. The duration of each request follows a negative exponential distribution with a mean value of 100 s. We consider that the source and destination nodes of a given request are randomly and uniformly chosen among the whole set of network nodes.

We consider IP requests with a fixed bitrate equal to 1/8 of the total lightpath capacity to avoid the capacity unfairness issue [33]. Indeed, high-bitrate requests tend to be blocked much more often than lower-bitrate requests, since they might not fit into the available trunk capacities.

At the optical layer, we assume that the fixed-alternate approach tries up to two alternate paths (2nd and 3^{rd}-shortest-paths as explained in Section 4) when an LSP setup is blocked, wherein the ingress node is responsible for reissuing the LSP setup [9]. At the IP layer, we

assume that the fixed-alternate approach has a centralized, complete knowledge of the network state as in traditional link-state routing, and up to two alternate paths are considered for the IP LSP setup. We also assume that the routing information at the IP layer is never stale or inaccurate.

The ant approach allows for up to 2 re-routing attempts at each node when a feasible route cannot be found [9,16] at both optical and IP layers.

We consider that the maximum number of hops allowed for ant or RSVP-TE messages is equal to the amount of bi-directional links existing on the physical topology.

For the DPA algorithm, we consider a hop limit H equal to 1.5, which minimized the blocking probability under moderate traffic loads. Note that if $H \leq 1$, the DPA policy becomes equivalent to the ANT-OLF policy.

For the failure scenarios, we consider a hold-off timer for starting the restoration at the IP layer T_{HO} equal to 1 s, which guarantees that the process for recovery at the optical layer is finished whereas not being too long to impact the IP layer.

The remaining simulation parameters, including AntNet's parameters, used in the simulations are the same as in [9].

5.1. Metrics

In this work, we use the following metrics to assess the proposed algorithms. The main metric is the blocking probability P_b, which accounts for the blocking probability of requests at the virtual topology. It is defined by the following expression:

$$P_b = \frac{C_{req}^{blocked}}{C_{req}^{est} + C_{req}^{blocked}} \tag{6}$$

where $C_{req}^{blocked}$ is the number of blocked IP requests and C_{req}^{est} is the number of successfully established IP connections.

The reconfiguration metric F is equal to the number of all released lightpaths over the simulation period T. We consider that a lightpath is released whenever the last IP LSP using it is finished. Thus, F can be used to assess the dynamics of the virtual topology over time. Moreover, higher values of F indicates that a fast switching time for the WXC is needed in order not to delay the lightpath setup.

The IP router port count metric P is equal to the average number of IP router ports used over the simulation period T. Since one IP router port is needed in each endpoint of a lightpath, thus the value of P is twice the average number of established lightpaths over T.

The physical topology utilization U_{PT} measures the average utilization of utilized bi-directional wavelength-links by the optical layer over the simulation period T. It is defined by the following expression:

$$U_{PT} = \int_0^T \frac{L(t)}{W \times M} dt \tag{7}$$

where $L(t)$ is the sum of all wavelengths utilized on each bi-directional link at time t and M is the total number of bi-directional links in the physical topology. As already mentioned before, for the CORONET CONUS topology, we have $M = 99$.

The virtual topology utilization U_{VT} measures the average utilization of all lightpaths by the IP layer over the simulation period T. It is defined by the following equation:

$$U_{VT} = \int_0^T \frac{A(t)}{B(t)} dt \tag{8}$$

where $A(t)$ is the sum of the bitrate of all active IP LSPs over all established lightpaths at time t and $B(t)$ is the sum of the capacity of all established lightpaths at time t.

The communication overhead accounts for the aggregated bandwidth used by the ants across all control channels. We assume that the ants are implemented as raw IP datagrams, which are composed of a 40-byte header and an 8-byte label for each WXC or IP router identifier.

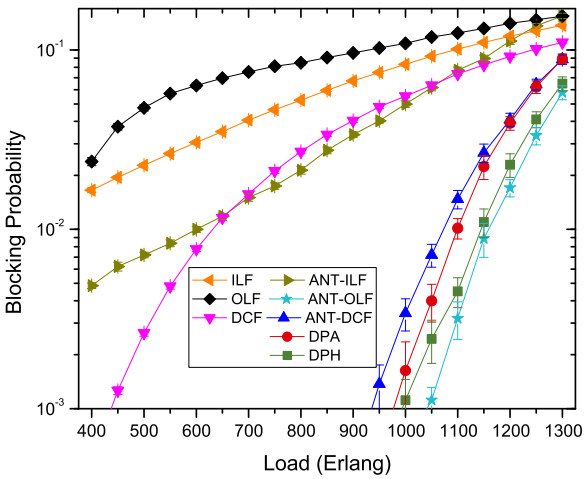

Fig. 1. Blocking probability for the NTTNet network with $W = 32$ wavelengths.

The setup time metric considers the time needed to successfully establish a lightpath or IP connection by using the RSVP-TE signaling protocol. Hence, it measures the transmission time at each traversed link along with the processing time at each traversed node needed for the *Path*, *Resv*, and eventual *PathErr* messages to set up a connection as detailed in [9,16].

The restorability metric R evaluates the resilience of the network in failure scenarios and it is defined by the following expression [34]:

$$R = \frac{C_{restored}^{failed}}{C^{failed}} \tag{9}$$

where $C_{restored}^{failed}$ is the number of connections affected by the failure(s) and restored by the recovery process and C^{failed} is the total number of connections affected by the failure(s).

Note that a connection cannot be restored if the failure takes place in its source or destination node. Thus, for the scenarios with node failures, the restorability may never be equal to 1.

6. Numerical results

First, we evaluate the fixed-alternate and ACO-based multilayer routing policies under normal operation of the network. In the following graphs, each plotted point is the average of 30 different runs, where each run executed 10^5 requests, and the error bar indicates the 95% confidence interval.

Fig. 1 shows that the ACO-based routing algorithm can outperform the fixed alternate routing policies, in terms of blocking probability. The best policy for fixed-alternate routing is DCF that has a performance more or less similar to the worst-performing ACO-based policy, which is ANT-ILF. The remaining ACO-based policies achieved comparable results, but ANT-OLF and DPH were the best policies in terms of the blocking probability. Indeed, similar to the results presented in [18], which were simulated with $W = 16$ wavelengths, we can observe that ACO-based policies have much lower blocking probability compared to fixed alternate routing policies until very high loads, where the blocking probability reaches levels above 10%.

Fig. 2 shows that all ACO-based routing policies, except ANT-ILF, can outperform the fixed-alternate routing in terms of blocking probability for IP LSP requests. ANT-OLF is the best performing ACO-based policy in terms of blocking probability for all network loads. DPH performs better at higher loads ($\geq$ 550 erlangs), while DPA and ANT-DCF perform better at lighter loads ($<$ 550 erlangs). The best policy for fixed-alternate routing is DCF, which attains a similar blocking probability performance of DPA and ANT-DCF at very high loads ($>$ 650 erlangs), where the blocking probability is already very high ($\approx$10%).

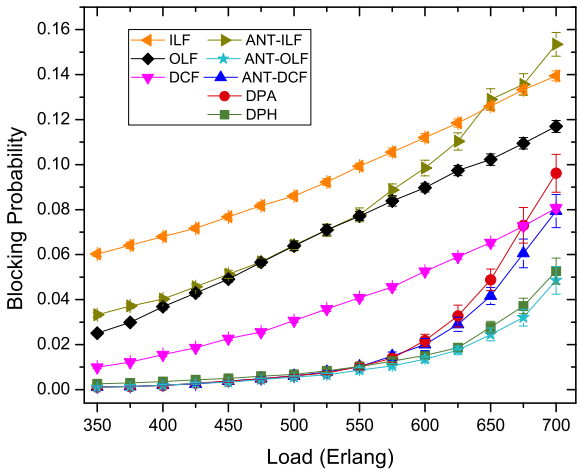

(a) Linear view

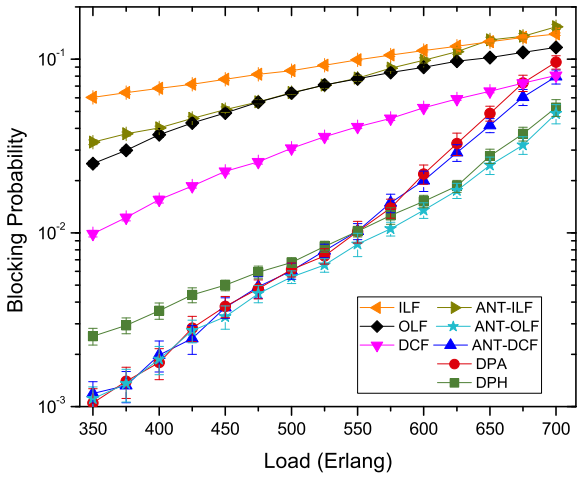

(b) Logarithmic view

Fig. 2. Blocking probability for the CORONET CONUS network with $W = 16$ wavelengths.

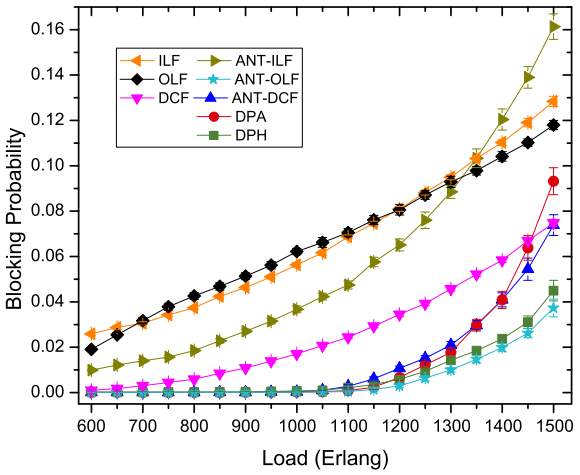

(a) Linear view

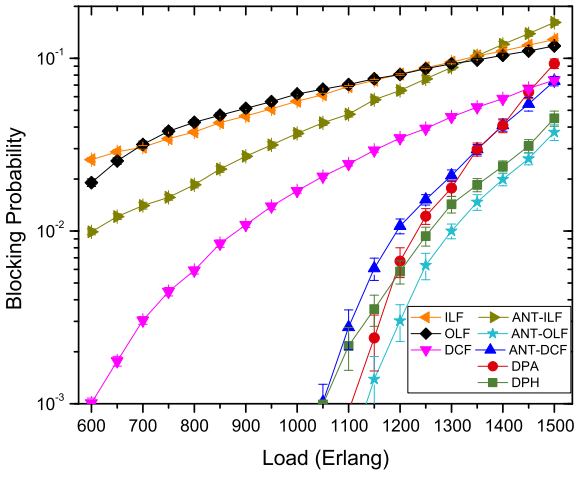

(b) Logarithmic view

Fig. 3. Blocking probability for the CORONET CONUS network with $W = 32$ wavelengths.

By doubling the number of wavelengths at each network link for the CORONET CONUS network as shown in Fig. 3, we can observe almost the same trend as depicted in Fig. 2, where ACO-based policies, except ANT-ILF, outperform the policies based on k-shortest path routing. The main difference is that the blocking probability of the OLF policy increases, becoming similar to the ILF policy when the number of wavelengths is doubled. The same effect can be observed when Fig. 1 and [18] are compared.

For sake of conciseness, the remaining metrics of this paper are simulated for the CORONET CONUS network considering only $W = 16$ wavelengths.

Fig. 4 shows that the virtual topology reconfiguration is a good indicator of the blocking efficiency when the algorithm class of the routing policy is considered. For instance, ANT-OLF achieves slightly higher values of VT reconfiguration among the ACO-based policies, becoming the best performing multilayer policy in terms of blocking probability. Correspondingly, DCF policy has the highest value of VT reconfiguration and the best performance among the fixed-alternate policies in terms of blocking probability. Moreover, ILF and ANT-ILF have the smallest values of VT reconfiguration and also the highest blocking probabilities among their counterparts. Hence, a more dynamic virtual topology results in less blocking.

In Fig. 5, the IP router port count needed for all policies is shown. As the load increases, the number of IP router ports also increases.

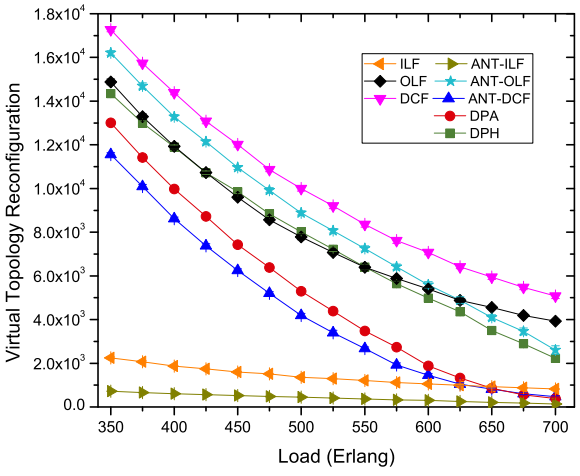

Fig. 4. Number of lightpath reconfigurations for the CORONET CONUS network ($W = 16$).

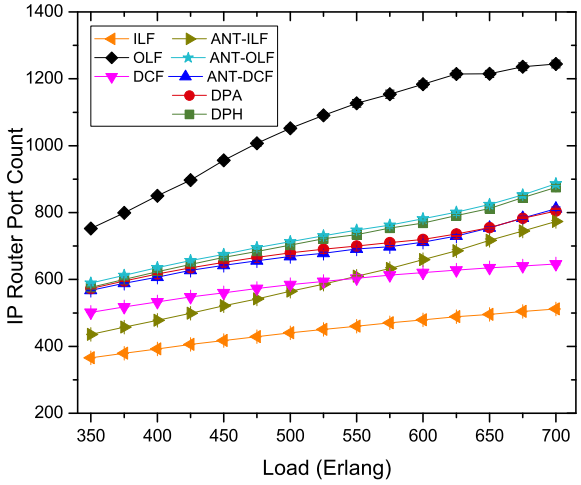

Fig. 5. Number of IP router ports for the CORONET CONUS network ($W = 16$).

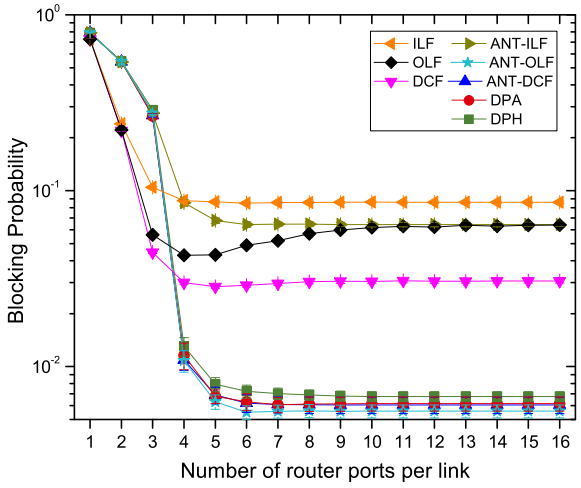

Fig. 6. Effect of the number of IP router ports on the blocking probability for the CORONET CONUS network ($W = 16$).

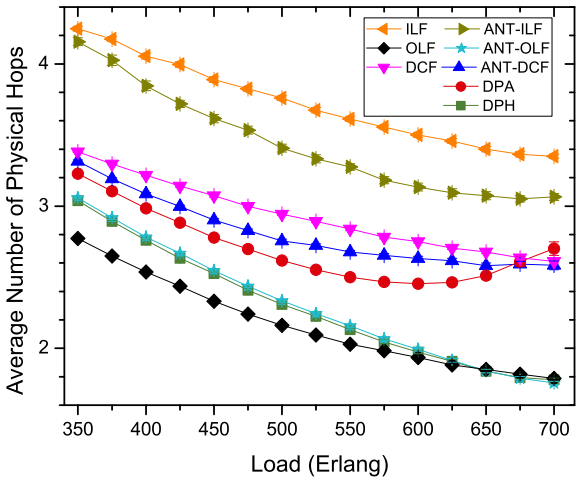

Fig. 7. Average number of physical hops for the CORONET CONUS network ($W = 16$).

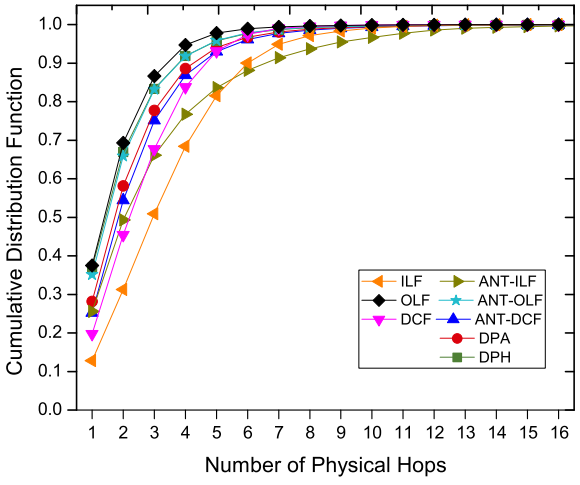

Fig. 8. Cumulative distribution of the number of physical hops for the CORONET CONUS network ($W = 16$).

The policies that favor the optical layer, such as OLF and ANT-OLF, establish more lightpaths at a given time. In effect, the OLF policy establishes much more lightpaths than the other policies. Conversely, the policies in their algorithm classes that favor the IP layer, such as ILF and ANT-ILF, establish fewer lightpaths. The remaining policies have IP router port counts that lie between those boundaries. Except for the OLF policy, we can observe that the number of used IP router ports is much smaller than the number of deployed IP router ports in the network, which is equal to $2 \times W \times M = 3168$.

The effect of the number of IP router ports per link on the blocking probability is shown in Fig. 6. We vary the number of IP router ports up to 16, which is the number of wavelengths deployed in each link. We consider the load of 500 erlangs, which is the load where the ACO-based policies, except for ANT-ILF, have a very similar performance in terms of blocking probability. As we can observe, the number of IP router ports needed to accommodate all traffic is much smaller than the number of deployed wavelengths in each link. Indeed, almost all policies have similar blocking performance until the number of IP router ports per link is equal to 6. We can also observe that ACO-based policies need a greater number of IP router ports than the fixed-alternate policies. For instance, when the number of IP router ports per fiber decreases from 4 to 3, the fixed-alternate policies outperform all ACO-based policies in terms of blocking probability.

The average number of hops for all policies can be seen in Fig. 7. As the load increases, requests for longer lightpaths are being blocked and, consequently, the established lightpaths become shorter in terms of the number of hops. The policies that favor the optical layer, such as OLF and ANT-OLF, tend to have fewer hops at the PT, while the policies that favor the IP layer, such as ILF and ANT-ILF, tend to have more hops at the PT. The remaining strategies have a number of physical hops that lie between those boundaries.

In Fig. 8, the cumulative distribution function of the number of physical hops for all policies is shown for the load of 500 erlangs. ACO-based policies tend to find a greater number of feasible, but longer routes in the PT than the fixed-alternate policies, which may help to lower the blocking probability, as seen in Fig. 2.

In Fig. 9, it is shown the probability of Ω being invoked first, i.e., when the IP layer is initially assigned to accommodate the LSP request. By definition, we have a 100% probability for the ILF and ANT-ILF policies and a 0% probability for the OLF and ANT-OLF policies. The DPH policy has a probability of approximately 15% to invoke Ω first, when the neighbor with the highest concentration of pheromone is found at the IP colony. The DCF and ANT-DCF policies have a probability ranging from 10% to 12% to invoke Ω first, when there is a direct lightpath between the source and destination nodes with enough capacity to serve the LSP request. Finally, the DPA policy has a probability ranging from 7% to 10% to invoke Ω first, when the

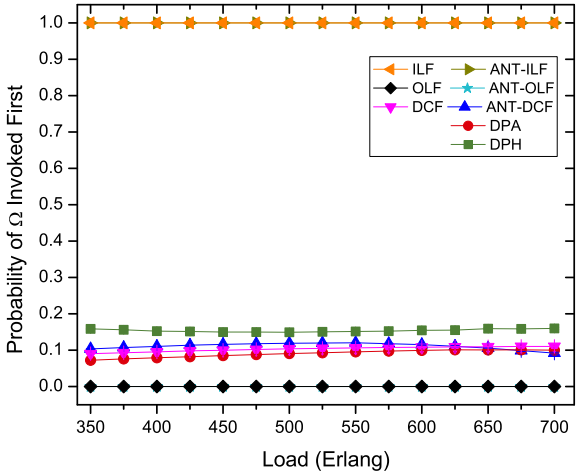

Fig. 9. Probability of Ω being invoked first for the CORONET CONUS network (W = 16).

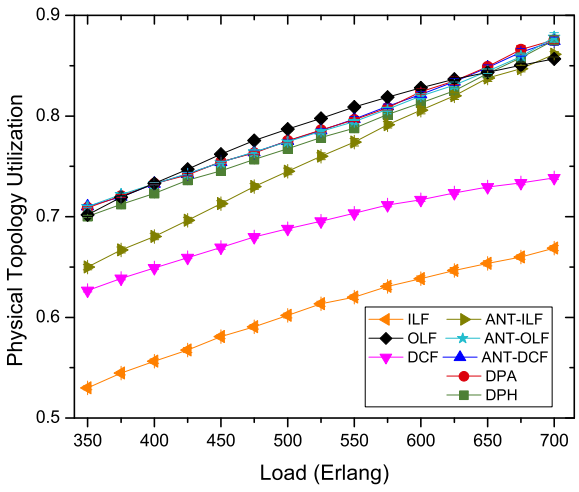

Fig. 10. Physical topology utilization for the CORONET CONUS network (W = 16).

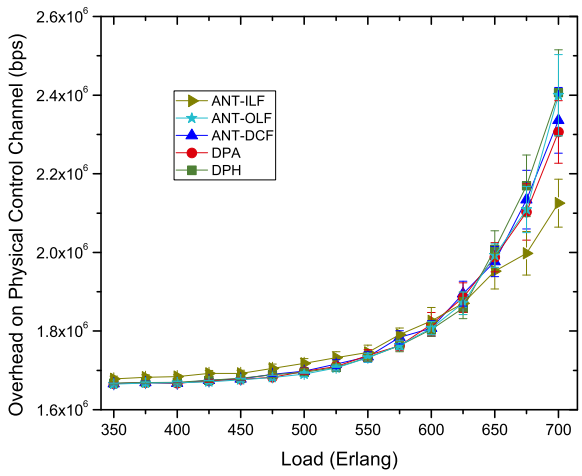

Fig. 11. Communication overhead at the optical layer for the CORONET CONUS network (W = 16).

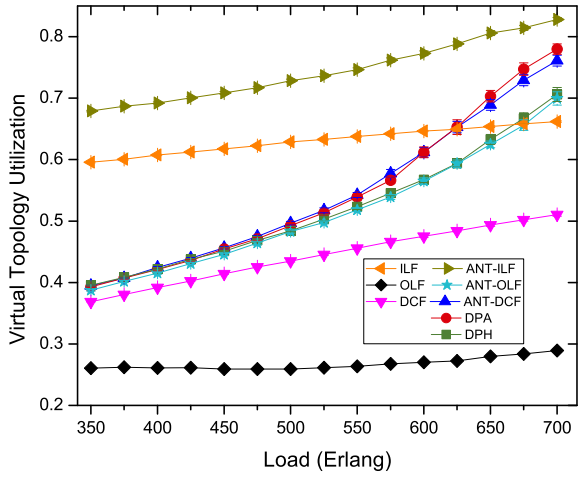

Fig. 12. Virtual topology utilization for the CORONET CONUS network (W = 16).

estimated path distance at the IP layer is less or equal than the hop limit H. Therefore, we can conclude that the DPA policy tends to favor the use of the optical layer more than the ANT-DCF and DPH policies, respectively.

Fig. 10 shows the utilization of the wavelength resources at the physical topology. We can observe that OLF and ANT-OLF are the policies in their algorithm classes with the highest pressure in the use of the resources of the optical layer. They have a similar utilization of the resources in the optical layer, which are closely followed by the ANT-DCF, DPA, and DPH policies. As expected, we can observe that ILF and ANT-ILF are the policies in their algorithm classes with the lowest pressure in the use of the resources of the optical layer. The ACO-based policies make better utilization of the physical topology than the fixed-alternate policies, except for the OLF policy, which may help to explain their better performance in terms of blocking probability.

The communication overhead of the ants in the WXC control channels of the entire network is depicted in Fig. 11. All ant-based policies have similar results. The aggregated bandwidth at the optical control plane ranges from 1 to 3 Mbps, which leads to an average overhead of around a few dozens kilobits at each individual control channel. In fact, the ants wandering in the network introduce very little overhead on the control channels, as already mentioned in [9]. At higher loads, the ants become more exploratory to find less congested routes, which cause a small increase in the communication overhead.

In Fig. 12, we can observe that ANT-ILF and ILF are the policies in their algorithm classes with the highest pressure on the use of resources at the IP layer, although they have the lowest pressure on the use of resources at the optical layer. In effect, the ANT-ILF and ILF policies do not take advantage of the resources at the optical layer as the others, but they have the IP layer with less free resources to allocate to the IP LSPs. Moreover, the remaining ACO-based policies make better utilization of the VT than the remaining fixed-alternate policies, which may also help to explain their better performance in terms of blocking probability.

In Fig. 13, it is shown that all ACO-based policies, except ANT-ILF, have a similar value for the number of virtual hops. As the load grows, for ACO-based policies, longer but less congested routes are selected, which increases the average number of virtual hops.

The cumulative distribution function of the number of virtual hops for all policies for the load of 500 erlangs can be observed in Fig. 14. As already mentioned, ACO-based policies increase the number of hops of the IP LSPs in order to find less congested routes.

Since the links in the VT may be composed of multiple physical hops, the aggregated communication overhead at the IP control plane tends to be smaller than the overhead seen at the optical control plane, as shown in Fig. 15. Actually, the communication cost for all IP router control channels due to ants is less than one megabit/s.

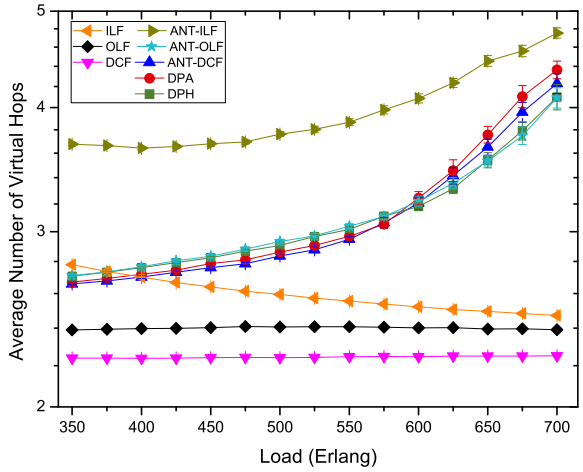

Fig. 13. Average number of virtual hops for the CORONET CONUS network ($W = 16$).

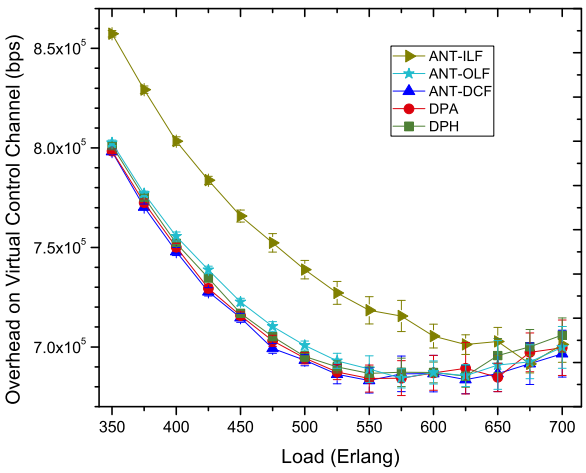

Fig. 15. Communication overhead at the IP layer for the CORONET CONUS network ($W = 16$).

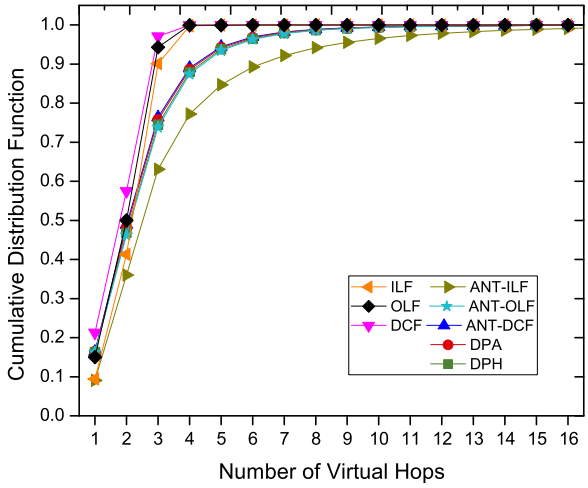

Fig. 14. Cumulative distribution of the number of virtual hops for the CORONET CONUS network ($W = 16$).

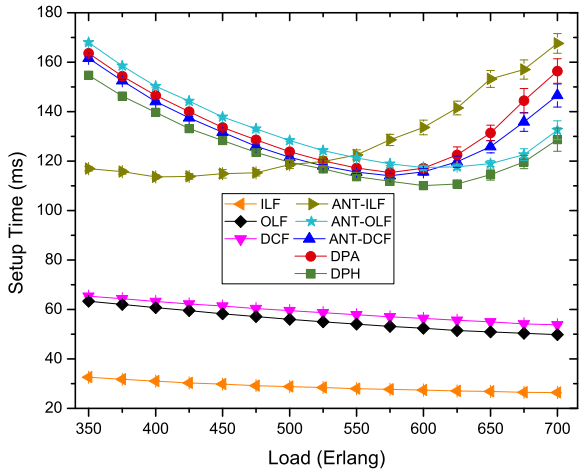

Fig. 16. Overall setup time for the CORONET CONUS network ($W = 16$).

All policies, except ANT-ILF, have similar results for the communication overhead in the VT. ANT-ILF has the highest communication overhead due to the greater number of virtual hops needed to establish the IP LSP connections.

As the load increases, the number of established lightpaths also increases. Consequently, the virtual topology becomes more connected and the ants can reach their destination in a smaller number of virtual hops, which results in a small decrease in the communication overhead at the IP control plane.

The overall setup time for an IP LSP connection can be observed in Fig. 16. For smaller loads and among the ACO-based policies, the ANT-ILF policy has the smallest value of setup time. Indeed, if an LSP request can be fulfilled without the intervention of the optical layer, which tends to occur more often in lighter loads, we can save time and, consequently, reduce the setup delay. Similarly, as the DPH policy invokes Ω more often, it has the best setup delay among the remaining ant-based policies. On the opposite side, as the ANT-OLF policy always requires the optical layer to fulfill an IP LSP request, it has the highest setup time for the lighter loads.

Also, note that for the ACO-based policies we have two opposing trends for the number of physical and virtual hops in the function of the load. As the load increases, the lightpaths are getting shorter whereas the IP LSP connections are getting longer in terms of the number of hops. For lighter loads, the effect of shorter lightpaths dominates and we can observe a decrease in the overall setup time. For higher loads, the effect of longer IP LSP connections combined with the need to invoke the crankback mechanism more frequently dominates and we can observe an increase in the overall setup time. Indeed, longer IP LSP connections at higher loads are especially important to explain the fast increase in the setup time of the ANT-ILF policy. On the contrary, the overall setup time for the fixed-alternate approaches decreases as the load grows since both the number of physical and virtual hops are getting smaller.

However, on average, ACO-based policies have setup times that range from two to three times the value for DCF and OLF policies, which are the best performing fixed-alternate policies in terms of blocking probability. Due to the fully distributed nature of the ACO algorithms, one can expect higher setup times compared to the proposed fixed-alternate approaches, which have a perfect global knowledge of the IP topology. This also explains the reason behind the ILF policy to have much lower setup time compared to OLF and DCF policies, whose setup times are dominated by the time spent on routing with crankback at the optical layer. Hence, at the IP layer, the fixed-alternate approaches can be seen as a lower bound for the setup time. Nonetheless, the setup times for ACO algorithms can be still considered reasonable enough for today's network requirements.

For evaluating the restoration performance of the fixed-alternate and ant-based multilayer routing policies under single network failure

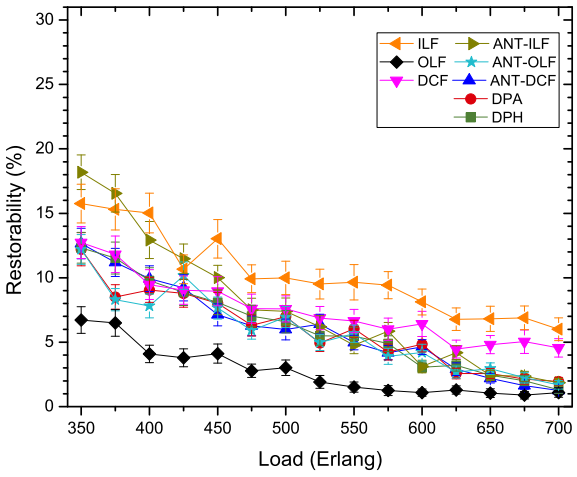

(a) Single-node failure

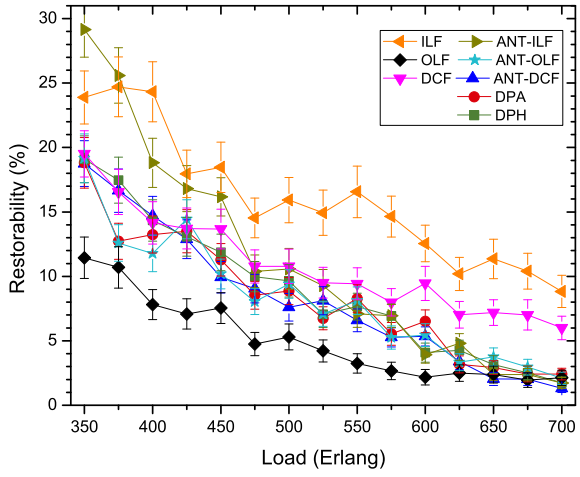

(b) Single-link failure

Fig. 17. Restorability at the optical layer for the CORONET CONUS network ($W = 16$).

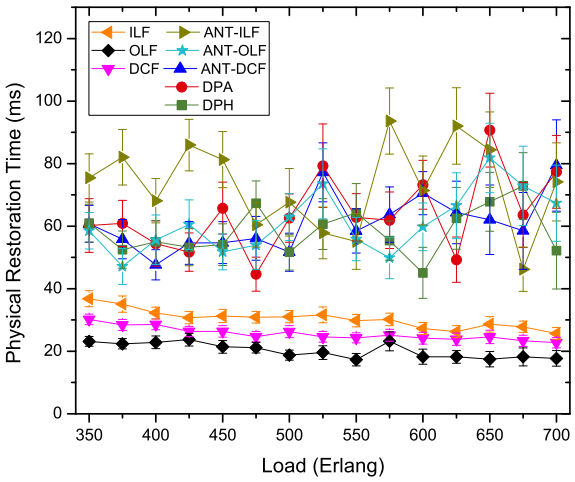

(a) Single-node failure

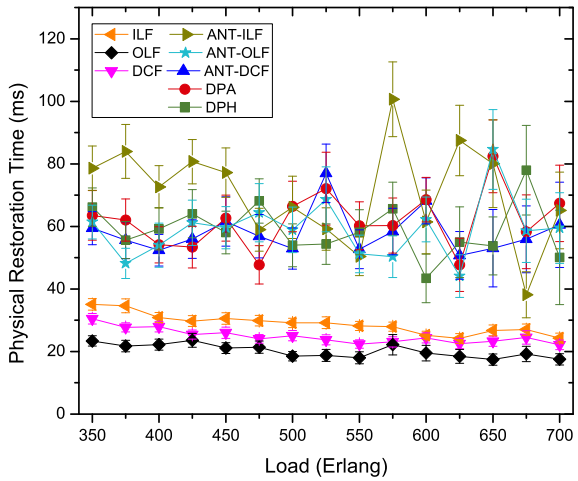

(b) Single-link failure

Fig. 18. Restoration time at the optical layer for the CORONET CONUS network ($W = 16$).

scenarios, we consider all possible single failures in four different times of the simulation in order to get a smaller margin of error. Each plotted point in the following graphs depicts the obtained average value and the error bar indicates the 95% confidence interval.

The restorability at the optical layer is shown in Fig. 17. As the ILF tends to use fewer resources on the optical layer, there are more available resources to restore lightpaths. Conversely, the aggressive use of optical network resources seen on the OLF policy leaves fewer spare resources on the optical layer, which leads to the smaller values of restorability. The remaining policies exhibit an intermediate performance, in terms of restorability, with similar results.

The restoration times at the optical layer for ACO-based policies are roughly the double than their fixed-alternate counterparts as depicted in Fig. 18.

In Fig. 19, we can observe that ACO-based policies are more efficient than fixed-alternate policies, restoring 50% to 100% more IP connections affected by a single-node failure after both IP and optical layer restoration process. For single-link failures, all ACO-based policies, except ANT-ILF, have restorability near 100%, while the fixed-alternate approaches have restorability from 80% to 60% at the same loads. It is important to note that the restorability in the optical layer is not directly correlated to the overall restorability of the IP connections.

The LSPs affected by a failure that could not be restored by optical layer are recovered by the IP layer after the hold-off timer T_{HO}. Fig. 20 considers the restoration time at the IP layer after T_{HO}. Topological policies have restoration times around 50 ms whereas ACO-based policies have restoration times starting at 120 ms for low loads going to 250 ms for higher loads. Again, due to the fully distributed nature of the ACO routing, one can expect much higher values for the restoration times compared to fixed-alternate routing with global state knowledge for the IP layer.

Table 2 summarizes the relative performance of each multilayer routing policies for the most important metrics used throughout this work. The relative performance is classified into four different categories, trying to make a qualitative assessment of the predominant behavior of the metrics as previously discussed in the text and presented in the figures. As a result, comparable results are classified in the same category, whereas dissimilar results are put in the maximum possible number of different categories.

In summary, we can conclude from the presented results that ANT-OLF is the best performing ACO-based policy. In general, it exhibits the smallest blocking probability and the highest overall restorability for single failures across all presented policies. It also exhibits lower communication overhead and lower restoration time among the ACO-based policies. Hence, for ACO-based policies, the best strategy is to always try to establish a lightpath before requesting an IP LSP connection. The rationale of this strategy is to provide the virtual topology

Table 2
Summary of the relative performance of each multilayer routing policy used throughout this work.

Metrics	Type[a]	ILF[b]	OLF[b]	DCF[b]	ANT-ILF[b]	ANT-OLF[b]	ANT-DCF[b]	DPA[b]	DPH[b]
Blocking probability	L	+	+	++	+	++++	+++	+++	++++
Lightpath reconfiguration	H	+	++++	++++	+	++++	+++	+++	++++
Router port usage	L	++++	+	+++	+++	++	++	++	++
Control overhead	L	NA	NA	NA	+++	++++	++++	++++	++++
Setup time	L	++++	+++	+++	++	++	++	++	++
Overall restorability	H	++	++	++	+++	++++	++++	++++	++++
Restoration time	L	++++	++++	++++	++	+++	+++	+++	+++

[a]H: Higher value is better; L: Lower value is better.
[b]++++: Excellent performance; +++: Good performance; ++: Average performance; +: Low performance.
NA: not applicable.

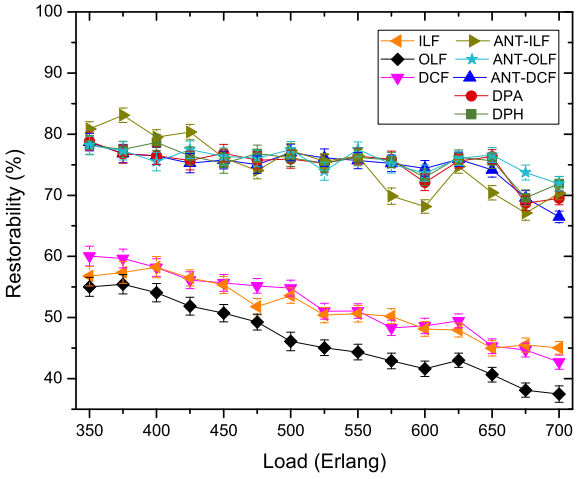

(a) Single-node failure

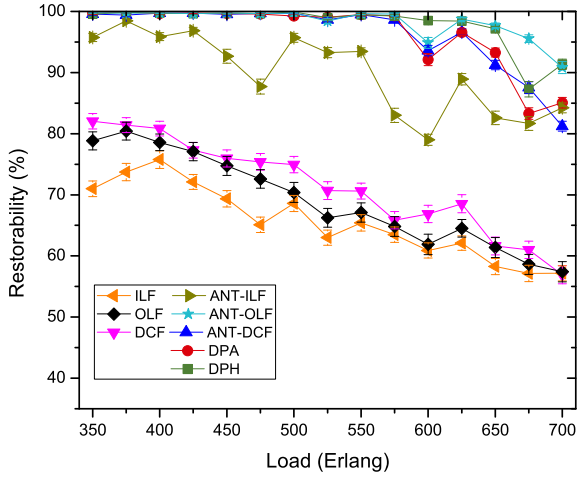

(b) Single-link failure

Fig. 19. Overall restorability for the CORONET CONUS network ($W = 16$).

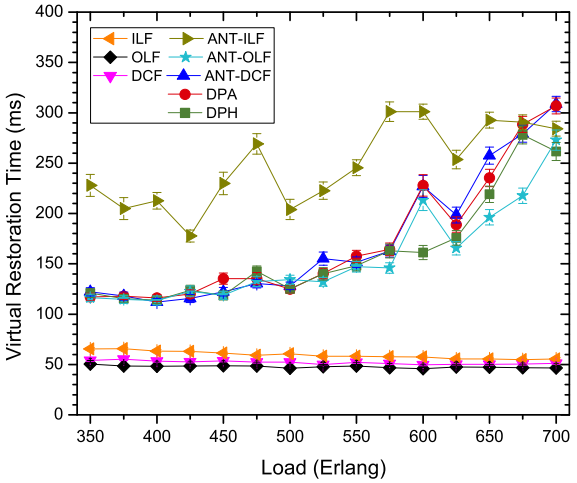

(a) Single-node failure

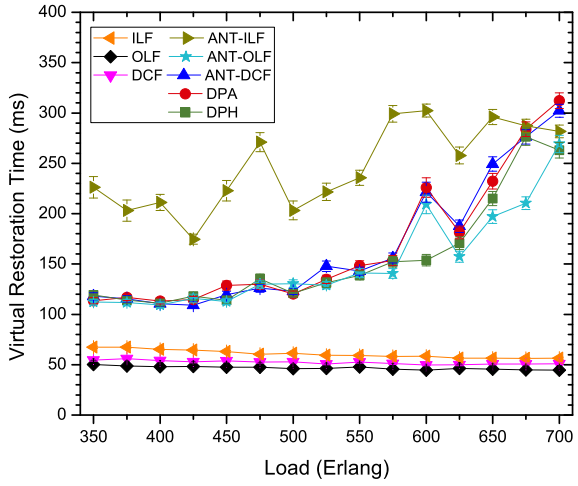

(b) Single-link failure

Fig. 20. Restoration time at the IP layer for the CORONET CONUS network ($W = 16$).

with the highest amount of capacity [21] so that it can be harnessed at the IP layer to find suitable connections. Furthermore, the ANT-OLF policy is based on the overlay model, which does not need to exchange information between control planes. Still, its main disadvantage is to have slightly higher setup times for lower loads among the ACO-based policies.

7. Conclusions

In this work, we have proposed the use of ACO-based routing algorithms as enabling technologies for coordinated cross-layer resource provisioning and restoration in IP/MPLS over optical networks. The proposed ACO-based routing policies assume disjoint control planes for each layer and only local routing information at each network node.

We have demonstrated that ACO-based routing policies can effectively coordinate the IP and the optical layers, even if little or no routing information is exchanged between the control planes of each layer. More specifically, we have shown that the proposed ACO-based routing policies can outperform fixed-alternate routing policies in terms of blocking probability and restorability of IP LSP connections in almost all cases while not incurring much higher setup and restoration times,

or noticeable communication overhead. In effect, ACO-based policies can better manage network resources than fixed-alternate policies.

However, it is important to point out that ACO-based policies require that AntNet-specific data structures and services to be maintained at each node and a larger number of IP router ports compared to the fixed-alternate policies, which can be a significant part of the network's Capital Expenditure (CAPEX).

CRediT authorship contribution statement

Kelvin Santos Amorim: Investigation, Methodology, Software, Validation, Visualization. **Gustavo Sousa Pavani:** Conceptualization, Supervision, Software, Validation, Data curation, Writing.

Declaration of competing interest

The authors declare that they have no known competing financial interests or personal relationships that could have appeared to influence the work reported in this paper.

Acknowledgments

This work was supported by São Paulo Research Foundation (FAPESP), Brazil, grant #2015/24341-7, and Conselho Nacional de Desenvolvimento Científico e Tecnológico (CNPq), Brazil, grant #237879/2012-3.

References

[1] A. Martinez, M. Yannuzzi, V. Lopez, D. Lopez, W. Ramirez, R. Serral-Gracia, X. Masip-Bruin, M. Maciejewski, J. Altmann, Network management challenges and trends in multi-layer and multi-vendor settings for carrier-grade networks, IEEE Commun. Surv. Tutor. 16 (4) (2014) 2207–2230.

[2] H. Zang, J.P. Jue, B. Mukherjee, et al., A review of routing and wavelength assignment approaches for wavelength-routed optical WDM networks, Opt. Netw. Mag. 1 (1) (2000) 47–60.

[3] G. Clapp, R.A. Skoog, A.C.V. Lehmen, B. Wilson, Management of switched systems at 100 Tbps: The DARPA CORONET program, in: International Conference on Photonics in Switching (PS), 2009, pp. 1–4.

[4] B. Ilia, A.W. Jackson, J. John, W.E. Leland, J.H. Lowry, W.C. Milliken, P.P. Pal, R. Subramanian, R. Kristin, C.A. Santivanez, D.M. Wood, PHAROS: An architecture for next-generation core optical networks, in: Next-Generation Internet: Architectures and Protocols, Cambridge University Press, 2011, pp. 154–178.

[5] M. Dorigo, T. Stützle, Ant Colony Optimization, MIT Press, 2004.

[6] G. Di Caro, F. Ducatelle, L.M. Gambardella, Theory and practice of ant colony optimization for routing in dynamic telecommunications networks, in: N. Sala, F. Orsucci (Eds.), Reflecting Interfaces: The Complex Coevolution of Information Technology Ecosystems, Idea Group, Hershey, PA, USA, 2008, pp. 185–216.

[7] F. Ducatelle, G. Di Caro, L. Gambardella, Principles and applications of swarm intelligence for adaptive routing in telecommunications networks, Swarm Intell. J. 4 (3) (2010) 173–198.

[8] Z. Zhang, K. Long, J. Wang, F. Dressler, On swarm intelligence inspired self-organized networking: Its bionic mechanisms, designing principles and optimization approaches, IEEE Commun. Surv. Tutor. 16 (1) (2014) 513–537.

[9] G.S. Pavani, H. Waldman, Routing and wavelength assignment with crankback re-routing extensions by means of ant colony optimization, IEEE J. Sel. Areas Commun. 28 (4) (2010) 532–541.

[10] C. Kyriakopoulos, G.I. Papadimitriou, P. Nicopolitidis, E. Varvarigos, Energy-efficient lightpath establishment in backbone optical networks based on ant colony optimization, J. Lightwave Technol. 34 (23) (2016) 5534–5541.

[11] Ítalo Brasileiro, I. Santos, A. Soares, R. Rabêlo, F. Mazullo, Ant colony optimization applied to the problem of choosing the best combination among m combinations of shortest paths in transparent optical networks, J. Artif. Intell. Soft Comput. Res. 6 (4) (2016) 231–242.

[12] A.S. Gravett, M.C. du Plessis, T.B. Gibbon, A distributed ant-based algorithm for routing and wavelength assignment in an optical burst switching flexible spectrum network with transmission impairments, Photonic Netw. Commun. 34 (3) (2017) 375–395.

[13] W. Guoli, Z. Qi, W. Houtian, T. Qinghua, Z. Wei, X. Xiangjun, Ant colony optimization based load balancing routing and wavelength assignment for optical satellite networks, J. China Univ. Posts Telecommun. 24 (5) (2017) 77–86.

[14] J. Mata, I. de Miguel, R.J. Durán, N. Merayo, S.K. Singh, A. Jukan, M. Chamania, Artificial intelligence (AI) methods in optical networks: A comprehensive survey, Opt. Switch. Netw. 28 (2018) 43–57.

[15] A. Farrel, A. Satyanarayana, A. Iwata, N. Fujita, G. Ash, Crankback signaling extensions for MPLS and GMPLS RSVP-TE, in: Request for Comments, IETF, 2007, RFC 4920 (Proposed Standard).

[16] G.S. Pavani, A.F. Queiroz, J.C. Pellegrini, Analysis of ant colony optimization-based routing in optical networks in the presence of byzantine failures, Inform. Sci. 340–341 (2016) 27–40.

[17] G. Di Caro, M. Dorigo, Antnet: Distributed stigmergetic control for communications networks, J. Artificial Intelligence Res. (1998) 317–365.

[18] K.S. Amorim, G.S. Pavani, Routing and restoration in IP/MPLS over Optical networks by means of ant colony optimization, in: IEEE Global Communications Conference, Globecom, 2019, pp. 1–6.

[19] C. Rožić, D. Klonidis, I. Tomkos, A survey of multi-layer network optimization, in: International Conference on Optical Network Design and Modeling, ONDM, 2016, pp. 1–6.

[20] W. Colitti, P. Gurzi, K. Steenhaut, A. Nowe, Adaptive multilayer routing in the next generation GMPLS Internet, in: 3rd IEEE International Conference on Communication, Systems, Software and Middleware, COMSWARE, 2008, pp. 768–775.

[21] M. Köhn, W. Colitti, P. Gurzì, A. Nowé, K. Steenhaut, Multi-layer traffic engineering (MTE) in grooming enabled ASON/GMPLS networks, in: Towards Digital Optical Networks, Springer, 2009, pp. 237–252.

[22] S. Koo, G. Sahin, S. Subramaniam, Dynamic LSP routing in IP/MPLS over WDM networks, IEEE J. Sel. Areas Commun. 24 (12) (2006) 45–55.

[23] B. Rajagopalan, J. Luciani, D. Awduche, IP over optical networks: A framework, in: Internet Request for Comments, 2004, pp. 1–48, RFC 3717 (Informational).

[24] P. Grassé, La reconstruction du nid et les coordinations inter-individuelles chez Bellicoitermes natalenis et Cubitermes sp. La théorie de la stigmergie: Essai d'interprétation des termites constructeurs, Insectes Sociaux 6 (1959) 41–81.

[25] E. Bonabeau, M. Dorigo, G. Theraulaz, Swarm Intelligence: From Natural to Artificial Systems, Oxford University Press, 1999.

[26] G.S. Pavani, H. Waldman, Traffic engineering and restoration in optical packet switching networks by means of ant colony optimization, Third International Conference on Broadband Communications, Network and Systems, BroadNets, San Jose, CA, 2006.

[27] E. Oki, K. Shiomoto, D. Shimazaki, N. Yamanaka, W. Imajuku, Y. Takigawa, Dynamic multilayer routing schemes in GMPLS-based IP+optical networks, IEEE Commun. Mag. 43 (1) (2005) 108–114.

[28] E. Salvadori, R. Lo Cigno, Z. Zsóka, Dynamic grooming in IP over optical networks based on the overlay architecture, Opt. Switch. Netw. 3 (2) (2006) 118–133.

[29] X. Niu, W.-D. Zhong, G. Shen, T.H. Cheng, Connection establishment of label switched paths in IP/MPLS over optical networks, Photonic Netw. Commun. 6 (1) (2003) 33–41.

[30] M. Pickavet, P. Demeester, D. Colle, D. Staessens, B. Puype, L. Depre, I. Lievens, Recovery in multilayer optical networks, J. Lightwave Technol. 24 (1) (2006) 122–134.

[31] P. Cholda, A. Jajszczyk, Recovery and its quality in multilayer networks, J. Lightwave Technol. 28 (4) (2010) 372–389.

[32] A. Chiu, G. Choudhury, G. Clapp, R. Doverspike, J.W. Gannett, J.G. Klincewicz, G. Li, R.A. Skoog, J. Strand, A.V. Lehmen, D. Xu, Network design and architectures for highly dynamic next-generation IP-over-optical long distance networks, J. Lightwave Technol. 27 (12) (2009) 1878–1890.

[33] S. Thiagarajan, A.K. Somani, Capacity fairness of WDM networks with grooming capabilities, Opt. Netw. Mag. 2 (3) (2001) 24–32.

[34] M. Clouqueur, W.D. Grover, Availability analysis of span-restorable mesh networks, IEEE J. Sel. Areas Commun. 20 (4) (2002) 810–821.

Kelvin Santos Amorim graduated from Technology College Termomecanica (FTT) in System Analysis and Development at Brazil, 2013. He received a Master degree in Information Engineering from Federal University of ABC in 2017. His interests include research on electronic communication protocols upon guided or unguided means and vulnerability exploring in well-established communication systems.

Gustavo Sousa Pavani graduated from University of Campinas (UNICAMP) in 2001 with a degree in Computer Engineering. He received his M.Sc. degree and his Ph.D. degree in Electrical Engineering from UNICAMP, in 2003 and 2006, respectively. Currently, he is an associate professor at Federal University of ABC (UFABC), Brazil. He has interest on the following topics: routing algorithms for packet-switched and circuit-switched optical networks by means ant-colony optimization (ACO), GMPLS control plane, and the optical network support for grid and cloud architectures.